ELSEVIER

Journal of Chromatography A, 926 (2001) 275–290

JOURNAL OF CHROMATOGRAPHY A

www.elsevier.com/locate/chroma

Long-term fate and persistence of the spilled Metula oil in a marine salt marsh environment Degradation of petroleum biomarkers

Zhendi Wang[a,*], M. Fingas[a], E.H. Owens[b], L. Sigouin[a], C.E. Brown[a]

[a]*Emergencies Science Division, ETC, Environment Canada, 3439 River Road, Ottawa, Ontario K1A 0H3, Canada*

[b]*Polaris Applied Sciences Inc., Bainbridge Island, WA 98110-2483, USA*

Received 12 March 2001; received in revised form 7 June 2001; accepted 14 June 2001

Abstract

Three coastal sites, heavily oiled from the 1974 Metula oil spill in the Strait of Magellan [two are salt marshes (East and West) and the third, an intertidal asphalt pavement], were examined during May 1998. Complete 'total oil analyses' were performed on the oil samples collected from these sites. Chemical fingerprinting data reveal, except for those samples from the East Marsh untreated plots which were only lightly to moderately weathered, that the spilled oil has undergone significant alteration in chemical composition after 24 years. There are no fundamental differences between the heavily weathered West Marsh and treated East Marsh samples. However, the effect of experimental filling action conducted in 1993 has been to substantially promote plant recolonization. The asphalt pavement samples indicate extremely high degradation of oil hydrocarbons, evidenced by a complete loss of *n*-alkanes from *n*-C_8 to *n*-C_{41} and by depletion of greater than 98% of the alkylated polycyclic aromatic hydrocarbon homologues. Even the most refractory biomarker compounds showed some degree of biodegradation. The biomarkers were generally degraded in the declining order of importance as follows: diasteranes>C_{27} steranes>tricyclic terpanes>pentacyclic terpanes>norhapanes~C_{29}-αββ-steranes.

Keywords: Oils; Petroleum; Polynuclear aromatic hydrocarbons; Alkanes; Terpanes; Steranes

1. Introduction

The oil tanker 'Metula', en route from the Arabian Gulf to Quintero Bay, Chile, ran aground during the night of 9 August 1974 on Banco Satelite, just to the west of the First Narrows in the Strait of Magellan, Chile. The vessel carried a cargo of 1.42 million barrels (194·106 kg) of light Arabian crude, of which about $50 \cdot 10^6$ kg were spilled along with 2×10^6 kg of Bunker C fuel during the period from 9 August to 25 September 1974. Approximately 250 km of coast were oiled, and the most heavily oiled sections were located on the south shore near the First Narrows between Punta Espora and Punta Anegada (Fig. 1). Between 1974 and 1993, no attempts were made to recover or treat the stranded oil, and oil that reached the shorelines of the Strait was left to weather naturally in this cold, marine [1] environment (the mean monthly air temperature ranges from 2.5°C to a maximum of 11.7°C in

*Corresponding author. Tel.: +1-613-990-1597; fax: +1-613-991-9485.

E-mail address: wang.zhendi@etc.ec.gc.ca (Z. Wang).

0021-9673/01/$ – see front matter
PII: S0021-9673(01)01051-2

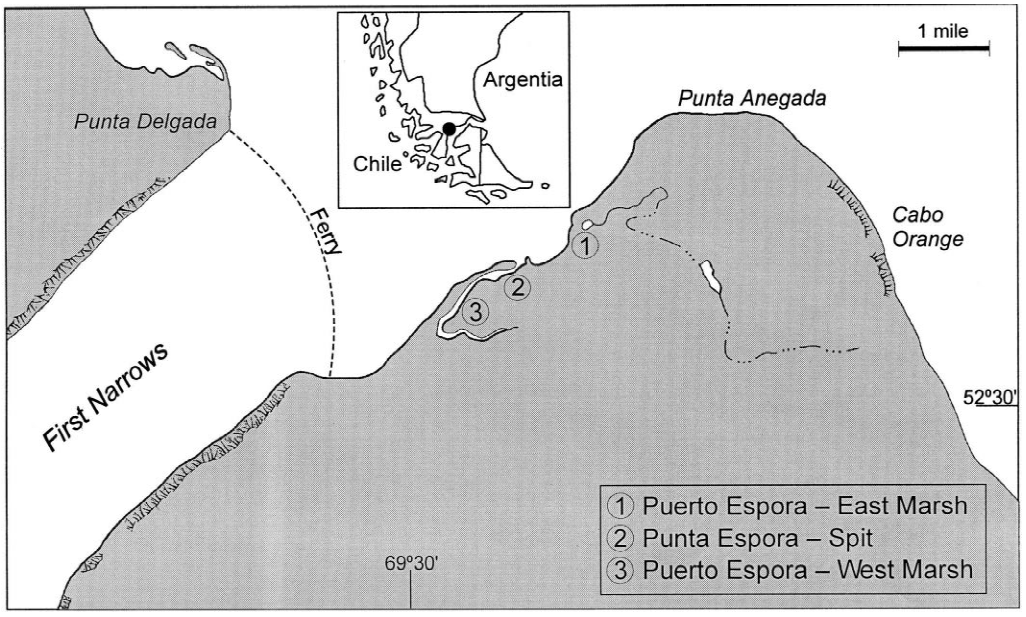

Fig. 1. Location of the 1998 Punta Espora study area of the 1974 Metula oil spill on the south shore of the Strait near the First Narrows between Punta Espora and Punta Anegada, Chile. The insert map shows the location of the 1974 Metula spill.

January, and strong westerly winds are characteristic throughout the year with wind velocities being frequently greater than 100 km/h).

A number of field surveys of the distribution of oil on the shoreline were conducted between August 1974 and 1987 [2]. A Universidad de Magallanes team visited the heavily oiled Puerto Espora East marsh (Site I in Fig. 1) in November 1990 and December 1991 [3] and subsequently conducted a series of small-scale field experiments at this site in January 1993 [4]. The treatment experiments included: tilling; application of fertilizer to the surface of the oil; and tilling with the fertilizer application on a set of 1 m^2 plots. A fourth plot was used as a control. The plots were triplicated and designated as 'A1–A4', 'B1–B4', and 'C1–C4' (control plots: A3/B1/C2; filling plots: A1/B2/C1; fertilizer plots: A2/B4/C4; and tilling plus fertilizer plots: A4/B3/C3). The plots were located at an elevation 50 cm below the spring high-tide level, and usually would be inundated by between 70 and 150 high tides each year [4].

The most recent field visit to the three coastal oiled sites in the Strait of Magellan was made by Owens et al. [2,5] during May 1998, 24 years after the spill event. They found that the majority of the oil on the open or exposed coast had been removed by natural processes. The only location with any large amounts of residual oil (surface and subsurface oil) was in Punta Espora area, where the oil was concentrated in three locations: two are salt marshes (East and West, Fig. 1) and the third is a large, continuous asphalt pavement formed on a mixed-sediment beach (sand, pebbles, and cobbles) in the inlet entrance to the West marsh (Site 2, Fig. 1). The objective of the 1998 study was to document oiling conditions and vegetative recovery in the area. At selected sites, samples of oiled sediment were collected for residual oil hydrocarbon analyses. The objectives of the analyses were (1) to quantitatively determine the chemical composition changes after 24 years exposure to weathering and biodegradation under these cold, marine environmental conditions, (2) to evaluate the degree to which the oil had been further weathered and degraded since the 1993 treatment experiments, (3) to determine the effectiveness of the different treatment methods on oil degradation, and (4) to establish reference points and benchmarks for possible future studies.

Site histories, details of the 1998 survey, and a

discussion of the long-term salt marsh recovery have been reported by Owens et al. [2,5]. This paper will focus on the analytical results and findings obtained. In particular, the persistence and degradation of biomarker compounds will be discussed.

2. Experimental

2.1. Materials and instruments

Distilled chromatographic solvents were used without further purification. Calibration standards used for determination of individual and total petroleum hydrocarbons (TPHs) include *n*-alkane standards from *n*-C_8 to *n*-C_{32} including pristane (*i*-C_{19}) and phytane (*i*-C_{20}), polycyclic aromatic hydrocarbon (PAH) standards (SRM 1491) from the National Institute of Standards and Technology (NIST), and biomarker (hopanes and steranes) standards from Chiron Laboratory of Norway [6,7].

Analyses for *n*-alkane distribution and TPHs were performed on a Hewlett-Packard (HP) 5890 gas chromatograph equipped with a flame-ionization detection (FID) system and an HP 7673 autosampler. Analyses of PAIR and biomarker compounds were performed on an HP Model 5890 GC equipped with a Model HP 5972 mass-selective detector. System control and data acquisition were achieved with an HP G1034C MS ChemStation.

2.2. Sample collection

A total of 14 samples was collected for analysis. Table 1 presents a detailed description of the samples. Eight samples were collected in the Puerto Espora East Marsh, including three from untreated control plots and five from treated plots (two from tilling, one from fertilizer application, and two from tilling with fertilizer application). Four samples were collected from the Puerto Espora West Marsh, and two representative samples were collected from the asphalt pavement area (Site 2, Fig. 1).

Due to the difficulty in obtaining a sample of the 1974 original oil, an Arabian light oil (AL-1991) from the Emergencies Science Division (ESD) collection originating from Chevron in 1991 was used as the reference oil in order to determine compositional changes of the Metula spill samples. This reference oil (AL-1991) was chosen because its

Table 1
Description of spilled Metula oil samples collected during the 1998 Field Visit (May 13–15, 1998)

Puerto Espora East Marsh plots samples	
EE-GO (grab oil)	Stiff black oil. Collected subsurface below the very hard crust.
EE-C1 (composite)	Collected from Control Plots A3/S1/C2, 3 sample composite of surface black crust.
EE-C2 (composite)	Collected from Control Plots A3/B1/C2, 3 sample composite of subsurface brown.
EE-T1 (tilling)	Collected from Tilling Plots A1/B2/C1, 3 sample composite of surface black crust.
EE-T2 (filling)	Collected from Tilling Plots A1/B2/C1, 3 sample composite of subsurface brown.
EE-F (fertilizer)	Collected from Fertilizer Plots A2/B4/C4, 3 sample composite of black-no-brown mousse.
EE-TF1 (tilling with fertilizer)	Collected from Tilling + Fertilizer Plots A1/B3/C3, 3 sample composite of surface black crust.
EE-TF2 (tilling with fertilizer)	Collected from Tilling + Fertilizer Plots A1/B3/C3, 3 sample composite of subsurface brown.
Puerto Espora West Marsh samples	
WE-P1	Plot 1, vertical composite to 5 cm depth.
WE-P2	Plot 2, vertical composite to 5 cm depth.
WE-RL (ropey lava)	Plot 1, surface oil cover.
WE-OL (old latex)Plot 1, surface oil cover.	
Puerto Espora asphalt pavement samples	
WI-1	West Inlet of West Espora. Pavement 12 cm thickness. Sample collected from 3 to 10 cm depth. Vertical composite.
WI-2	West Inlet of West Espora. Pavement 12 cm thickness. Sample collected from 3 to 10 cm depth. Vertical composite.

chromatographic fingerprint was very similar to that of the original Metula oil [8].

2.3. Sample extraction, cleanup and analysis

The Metula samples (60–130 g) were weighed, placed in 250-ml solvent-rinsed Erlenmeyer flasks, spiked with the appropriate surrogates (*o*-terphenyl, and a mixture of [$^2H_{10}$]acenaphthene, [$^2H_{10}$]phenanthrene, [$^2H_{12}$]benz[*a*]anthracene, and [$^2H_{12}$]perylene), and mixed with 100 g of sodium sulphate to dry the samples. If the sample had excessive moisture, additional amounts of sodium sulphate were added. The samples were then serially extracted three times with 150 ml of dichloromethane (DCM) for 30 min each time using sonication (50/60 Hz, 150 W). If there was visible colour in the third extraction, an additional extraction was performed. It was noted that most samples were very high in clay content. The extracts were combined, dried with sodium sulphate, and then filtered though sodium sulphate on a layer of glass wool. The extracts were concentrated to appropriate volumes and solvent-exchanged with hexane by means of rotary evaporation and further concentrated under nitrogen. An aliquot of the concentrated extract was evaporated with N_2 to a residue and weighed on a microbalance to obtain a total solvent extractable material mass (TSEM, expressed as mg/g of sample). The reference source Arabian oil was directly dissolved in hexane at a concentration of 100 mg/ml, and an aliquot of the solution containing ~15 mg of oil was spiked with the appropriate surrogates prior to the column cleanup.

A microcolumn packed with 3 g of activated silica gel and topped with 0.5 cm anhydrous sodium sulfate was employed for sample cleanup and fractionation of the oil. The column was conditioned with 20 ml of hexane. Appropriate aliquots of the concentrated extracts containing ~15 mg of TSEM were then quantitatively transferred onto the column. Hexane (12 ml) was used to elute aliphatic hydrocarbons, and 15 ml of 50% (v/v) benzene in hexane was used to elute aromatic hydrocarbons. Half of the hexane fraction (F1) was used for analysis of saturates and biomarker compounds; half of 50% benzene fraction (F2) was used for analysis of alkylated PAH homologues and other US Environmental Protection Agency (EPA) priority PAHs. The remaining half of F1 and F2 were combined (F3) and used for determination of total GC-detectable TPH, GC-resolved hydrocarbons, and the GC-unresolved complex mixture of hydrocarbons (UCM). These three fractions were concentrated to appropriate volumes (~0.4 ml), spiked with appropriate internal standards (50 μl of 200 ppm 5α-androstane and 50 μl of 20 ppm C_{30}-ββ-hopane, 50 μl of 10 ppm [$^2H_{14}$]terphenyl, and 50 μl of 200 ppm 5α-androstane for Fl, F2, and F3, respectively), and then adjusted to an accurate preinjection volume (0.50 ml) for GC–FID and GC–MS analyses. For detailed chromatographic conditions, analysis quality control, and quantification methodology, refer to Refs. [6,7].

3. Results and discussion

3.1. Fingerprints of hydrocarbons and hydrocarbon groups in residual oil

Assessment of the degradation and weathering trends of different Metula sample groups can be illustrated by qualitative and quantitative inspection of their GC fingerprints [7,9–16]. Fig. 2 shows the GC–FID chromatograms for the reference source Arabian oil and four spilled oil samples representing samples of the East Marsh control plots, the East Marsh treated plots, West Marsh, and the asphalt pavement, respectively. Figs. 3 and 4 depict the *n*-alkane distribution and PAH fingerprints for these representative samples, respectively. Table 2 summarizes chemical analysis results of major hydrocarbons and hydrocarbon groups in residual oil. Note that to quantitatively compare the composition changes of the residual oil, all data discussed below are expressed relative to the amount of TSEM rather than to the sample mass. That is, comparison of samples is based on the mass of residual oil in the samples.

Examination of the fingerprinting results permits classification of the Puerto Espora samples into three groups according to the extent and degree of the oil weathering and degradation processes (Table 2).

(a) Less degraded East Marsh control samples from the untreated area: The three samples (EE-GO, EE-C1 and EE-C2) from the untreated locations have

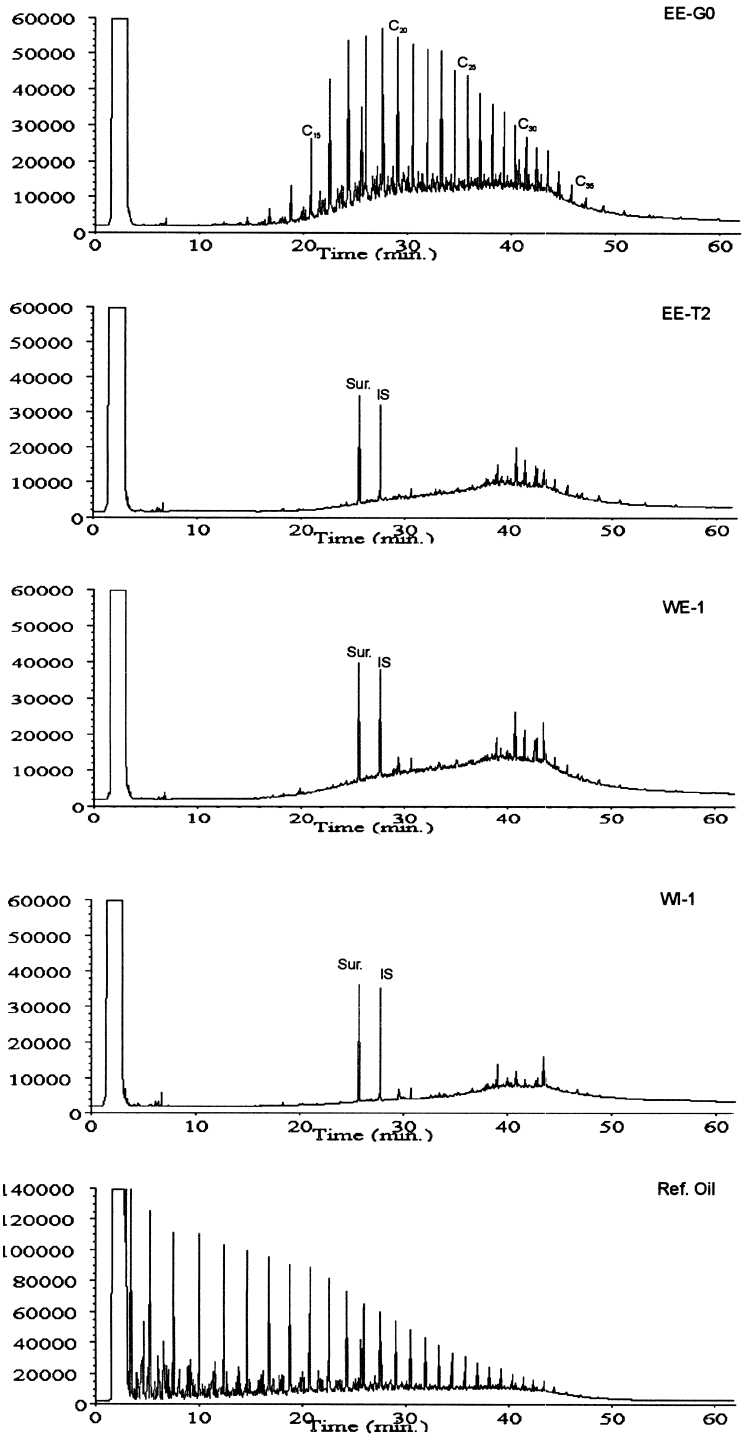

Fig. 2. Comparison of GC–FID chromatograms for total petroleum hydrocarbon (TPH) and *n*-alkane analysis of the reference Arabian Light oil (bottom) and the samples EE-GO, EE-T2, WE-1, and WI-1, representing the less degraded East Marsh controlled plots samples, the heavily degraded East Marsh treated and West Marsh untreated samples, and the most degraded asphalt pavement samples, respectively. I.S.: Internal standard 5-α-androstane and Sur: surrogate *o*-terphenyl. Note that different *y*-axis scale is applied for the reference oil.

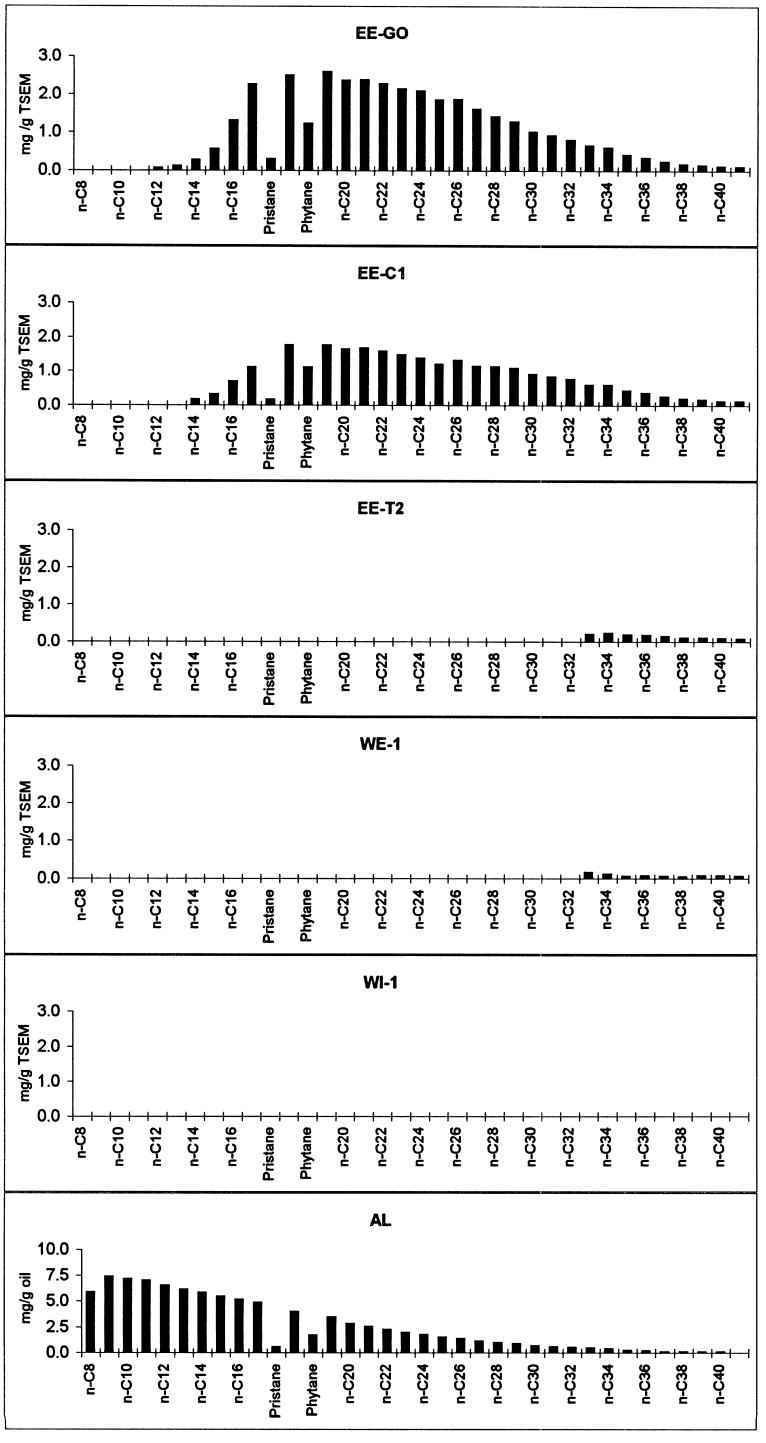

Fig. 3. *n*-Alkane distribution of the Metula spill oil. EE-GO and EE-C1, EE-T2 and WE-1, and WI-1 represent the East Marsh untreated plot samples, the East Marsh treated and West Marsh untreated plot samples, and the asphalt pavement samples, respectively. AL is the reference Arabian Light oil. Note that different *y*-axis scale is applied for the reference oil.

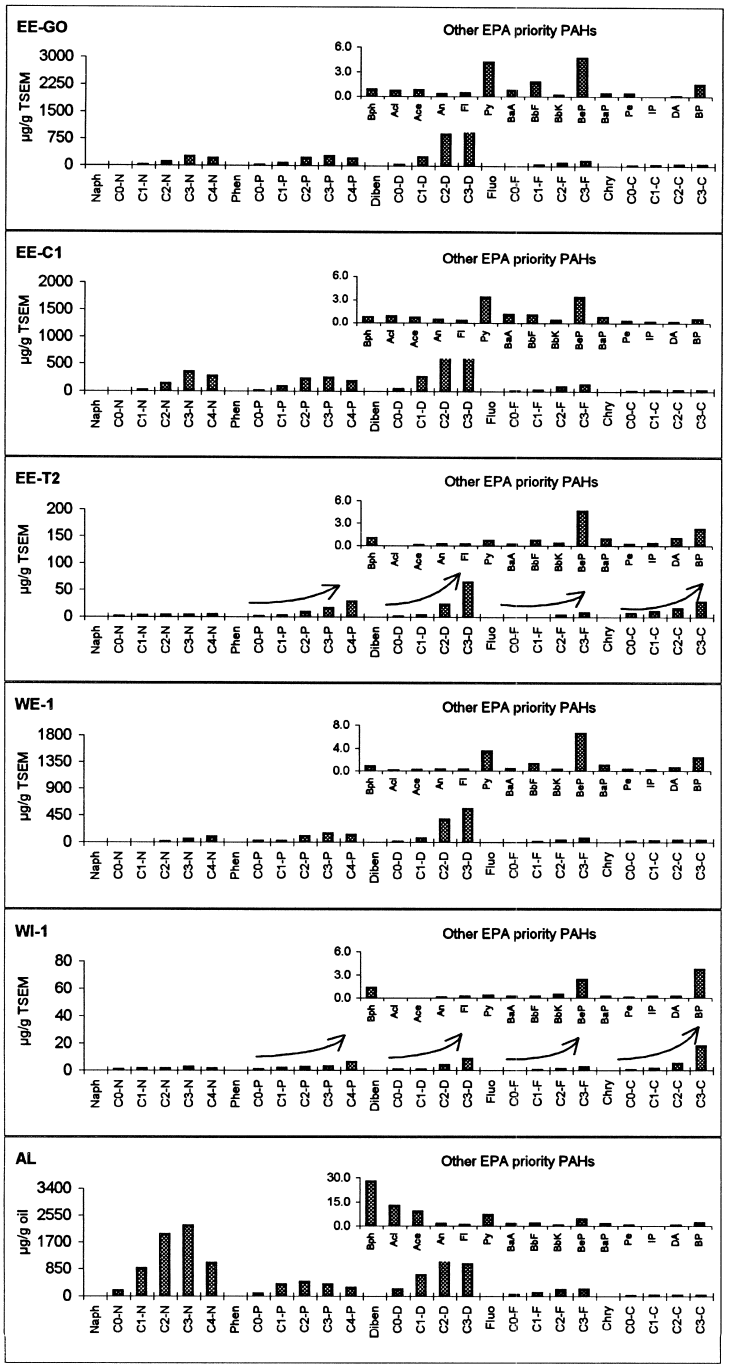

Fig. 4. Fingerprints of target alkylated PAHs of the Metula spill oil samples (EE-GO and EE-C1, EE-T2 and WE-1, and WI-1). For clarity, different *y*-axis scales are applied for different samples. N, P, D, F, and C represent naphthalene, phenanthrene, dibenzothiophene, fluorene, and chrysene, respectively; 0–4 represent carbon number of alkyl groups in alkylated PAH homologues. The left inserts are enlarged fingerprints of the other EPA priority PAHs. The abbreviations from Bph to BgP for the other EPA priority PAHs represent biphenyl, acenaphthylene, acenaphthene, anthracene, fluoranthene, pyrene, benz[*a*]anthracene, benzo[*b*]fluoranthene, benzo[*k*]fluoranthene, benzo[*e*]pyrene, benzo[*a*]pyrene, perylene, indeno[1,2,3-*cd*]pyrene, dibenz[*a*,*h*]anthracene, and benzo[*ghi*]perylene, respectively. The arrows indicate the compositional changes of $C_0 - < C_1 - < C_2 - < C_3 - < C_4 -$ in the target alkylated PAH homologous series.

Table 2
Summary of hydrocarbons and hydrocarbon groups analysis results

Analysis parameters	Samples from Puerto Espora East Marsh untreated area and control plots (sample = 3)	Samples from Puerto Espora East Marsh treated plots (sample = 5)	Samples from Puerto Espora West Marsh untreated plots (sample = 4)	Puerto Espora asphalt pavement samples (sample = 2)	Reference Arabian Light Oil
TSEM (mg/g dried sediment)	558–827	34–555	99–233	12–17	–
GC−TPH (mg/g TSEM)	300–380	180–290	200–300	122–133	535 (mg/g oil)
Resolved peaks					
GC–TPH	0.13	0.04–0.05	0.04–0.05	0.04	0.26
Saturates/TPH (%)	74–79	66–72	60–70	70–71	81
Aromatics/TPH (%)	21–26	28–34	30–40	29–30	20
Total *n*-alkanes[a] (mg/g TSEM)	22–36	1.1–7.4	0.7–1.2	0.0–0.3	90 mg/g oil
Lowest low-end *n* -alkane	*n*-$C_{12}/C_{14}/C_{16}$	*n*-$C_{18}/C_{27}/C_{30}/C_{33}$	*n*-$C_{30}/C_{31}/C_{32}/C_{33}$	none/*n*-C_{37}	*n*-C_8
Total of Alkylated PAHs[b] (μg/g TSEM)	3200–4000	615–2730	550–2890	60–150	11367 μg/g oil
Ratio of alkylated chrysenes to the sum 5-alkylated PAH series	0.02–0.03	0.04–0.25	0.05–0.14	0.29–0.39	0.01
Total of target biomarkers[c] (μg/g TSEM)	1400–1700	1766–2100	1932–2300	550–980	1089 μg/g oil
Conc. of C_{30}αβ-hopane (μg/g TSEM)	270–305	340–420	380–460	60–130	210 μg/g oil
Ratio of biomarkers to *n*-alkanes	0.05 –0.07	0.3–1.9	1.7–2.9	>3.7	0.01
Weathered[d] (%)	25–32	40–50	46–55	The most degraded	–

[a] *n*-Alkanes include *n*-C_8–*n*-C_{41} plus pristane and phytane.
[b] Alkylated PAHs include alkylated naphthalene (C_0–C_4), phenanthrene (C_0–C_4), dibenzothiophene (C_0–C_3), fluorene (C_0–C_3), and chrysene (C_0–C_3) homologous series.
[c] Target biomarkers include C_{23} and C_{24} tricyclic terpanes, C_{29}-αβ-norneohopane and C_{30}-αβ-hopane, C_{31}–C_{35} homohopane series with 22S- and 22R-17α(H), 21β(H) configuration, Ts and Tm, and C_{27} and C_{29}-αββ-steranes.
[d] The weathered percentages of the residual oil were determined using C_{30}-αβ-hopane as the internal conservative reference.

the highest TPH values, significantly higher ratio values of resolved saturate peaks to the total saturates (Fraction 1) and resolved hydrocarbon peaks to TPH (Fraction 3) relative to all of the other samples. These three samples also demonstrated the presence of highly-abundant *n*-alkanes and isoprenoid compounds starting from *n*-C_{12} (22 to 36 mg of *n*-alkanes per gram TSEM) and higher concentrations of the target PAHs including the 5 alkylated PAHs (alkylated, C_0- to C_4-, naphthalene, phenanthrene, dibenzothiophene, fluorene, and chrysene homologous series) and other EPA priority unsubstituted PAHs (note: see Fig. 4 for the definition of the other EPA priority PAHs). These observations clearly indicate that East Marsh control plot oil experienced less weathering and biodegradation.

(b) Heavily degraded samples from East Marsh treated plots and West Marsh untreated plots: The oil samples from the East Marsh treated plots were much more heavily degraded than the oil samples from the untreated control plots, characterized by the following chromatographic features: (1) TPH values were significantly lower, with no alkanes lighter than *n*-C_{27} in four of the five samples; (2) Pronounced large unresolved complex mixture (UCM) ‘humps’ in GC chromatograms were evident; (3) No lighter BTEX (benzene, toluene, ethylbenzene, and xylenes) and alkylbenzene compounds were detected; (4)

Striking decreases in the abundance of alkylated naphthalenes were very apparent (greater than 90% of naphthalene series were lost) in comparison with the reference oil and East Marsh untreated plot samples,. Also, development of a composition change profile of $C_0-<C_2-<C_2-<C_3-$ in each alkylated PAH group was very clear; (5) The relative percentage of biodegradation-resistant chrysene series in the total 5 alkylated PAH series exhibited a significant increase (increased to 0.04–0.25 from 0.01 for the reference oil). At the same time, decreases in the relative ratios of the sum of the alkylated naphthalenes, phenanthrenes, dibenzothiophenes, and fluorenes to the sum of the alkylated chrysenes were pronounced as well; (6) Biodegradation of oil in the samples clearly occurred, evidenced by the dramatic alteration in the relative distribution of characteristic PAH isomers 4-: 2-/3:- 1-methyldibenzothiophene and ratios of (3-+ 2-methylphenanthrene) to (4-/9-+l-methylphenanthrene) [16–19].

In terms of environmental conditions such as mean monthly temperature range, wind velocities, and mean tidal range [1], both locations (East and West Marshes) are similar. However, the samples from the untreated West Marsh plots showed very different degradation trends from the untreated East Marsh plots samples (WE-1 vs. EE-C1), but very similar degradation trends with the samples from treated East Marsh plots (WE-1 vs. EE-T2). None of the four West Marsh samples had *n*-alkanes lighter than *n*-C_{30}. Heavy loss of the oil-characteristic alkylated PAH homologues and other EPA priority PAHs was obvious. This observation may suggest rather similar abiotic weathering, but much greater biodegradation for the West Marsh plot samples than the untreated East Marsh samples.

Although the state of the oiled-beach restoration technology is primitive, it should be emphasized that the treatments applied to the East Marsh plots significantly promoted weathering and biodegradation of the spilled oil. The experimental plots that were tilled in 1993 have the most weathered oil of all the samples collected in the two marsh study areas, as discussed above. Plant count data [1,5] from the East Marsh tilled plots and the adjacent untreated area clearly indicate that tilling substantially increased the plant recolonization. This increase implies that recovery of the marshes almost certainly would have been accelerated, had tilling or mixing been conducted on these sites after the spill.

(c) The most degraded Punta Espora Backbeach samples: The results of the GC analyses on the two samples collected from the asphalt pavement showed that these were more degraded than all other samples collected during this study (Table 2). The samples demonstrated the following compositional features: the lowest GCTPH values; the highest content of asphaltenes plus polars; the lowest values of resolved peaks to GCTPH and the highest UCM/TPH values; the lowest concentrations of the total *n*-alkanes (one sample had no *n*-alkanes and isoprenoid compounds detectable up to *n*-C_{41} and the other sample had no *n*-alkanes lighter than *n*-C_{37}); trace levels of the total 5 alkylated PAH series; and the highest ratio values of the total target biomarkers to the total *n*-alkanes (>3.7). Greater than 99% alkylated PAHs were lost for these two samples in comparison with the reference Arabian oil. A profile showing the compositional changes of $C_0-<C_1-<C_2-<C_3-<C_4-$ in each target alkylated PAH homologous series is very apparent (Fig. 4). Also, there was evident degradation of the chrysene series, with concentrations of only 24 and 44 μg/g TSEM, whereas values for other samples were in a range from 63 to 130 μg/g TSEM. More importantly, these two samples showed significant degradation of biomarker compounds (which will be discussed later), further indicating extremely high degradation of the asphalt pavement samples.

3.2. Degradation of biomarker compounds

Biomarker compounds are highly biodegradation−resistant and have been widely used in geochemistry for studying ancient sediments, thermal maturity of petroleum, and oil–oil correlations [20–22]. In recent years, they have been increasingly used for the purpose of source identification and differentiation of oils, and monitoring the weathering and degradation process of oils under a wide variety of environmental conditions [12,16,21,23–28]. However, under severe weathering conditions biomarkers are also biodegradable. Therefore, comparison of the relative amounts of biomarker can be also used to rank oils as to the extent of biodegradation because

of their differential resistance to biodegradation [29–32]. For example, Peters and Moldowan have created a 'quasi-stepwise' sequence for assessing the extent to which an oil has been biodegraded, based on the relative abundances of the various biomarker hydrocarbon classes [20].

Fig. 5 shows the mass fragmentograms at *m/z* 191 for the most weathered sample WI-1 from the asphalt pavement, the less degraded sample EE-GO from the East Marsh untreated plots, and the reference oil. It can be seen from Fig. 5 that the mass fragmentograms of the reference oil and sample EB-GO are characterized by the distribution in a wide range from C_{21} to C_{35} terpanes with pentacyclic C_{29}-αβ-norhopane and C_{30}-αβ-hopane being the most prominent. The distribution pattern of the sample EE-GO is nearly identical to that of the reference oil AL-1991. No obvious sign of biomarker degradation is observed for sample EE-GO. The degradation of biomarker terpanes, however, is very apparent in

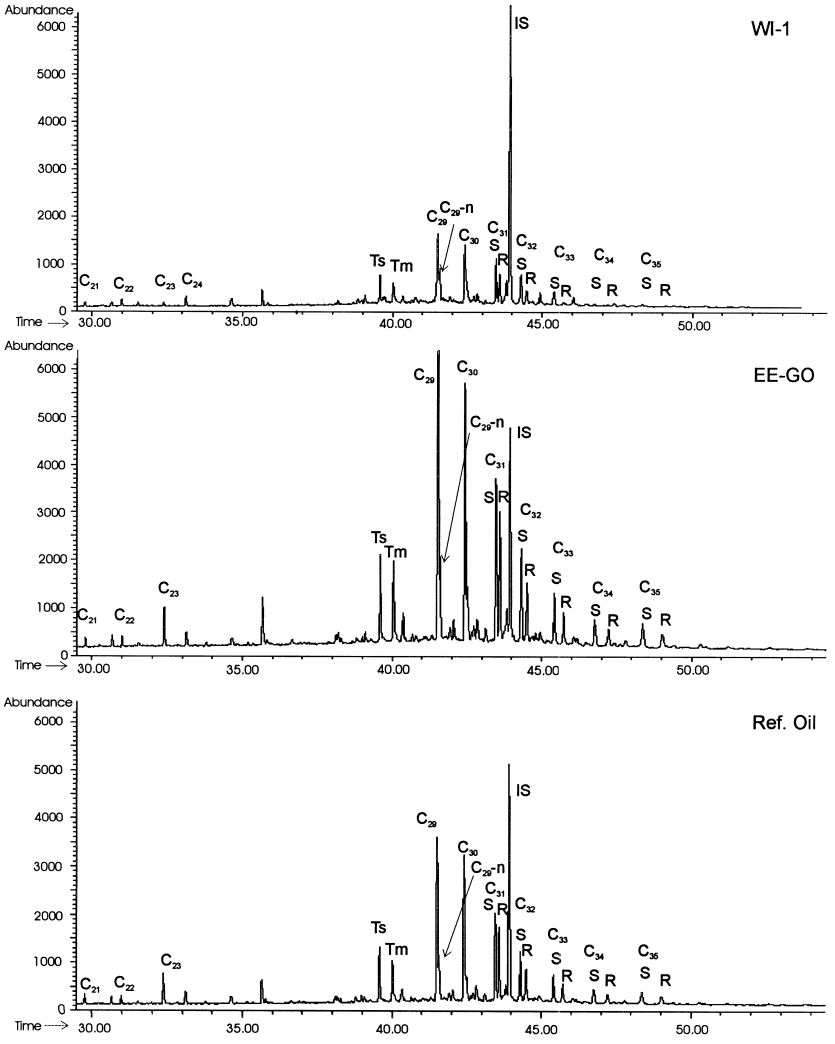

Fig. 5. GC–MS fragmentogram at *m/z* 191 of terpanes from the most degraded oil sample WI-1 (top), the less degraded oil sample EE-GO (middle), and the reference oil (bottom) after 24 years of weathering. I.S.: internal standard C_{30}-ββ-hopane). Refer to Table 3 for the full names of these terpane compounds shown in this figure. Time scales in min.

sample WI-1. The concentrations of all target biomarkers determined are significantly smaller than the corresponding biomarkers in the reference oil (550 μg/g TSEM vs. 1089 μg/g oil, Table 2).

For the αβ-homohopane (C_{31}–C_{35}) series (with 22S- and 22R-stereochemistry), heavier hopane homologues were observed to be more readily biodegraded than the lighter ones in a degradation sequence of $C_{35}>C_{34}>C_{33}>C_{32}>C_{31}$ with the degradation of the 22R epimers being preferential. As Fig. 5 shows, the pairs of heavier hopane homologues C_{35} and C_{34} homohopane epimers (22S and 22R) of the sample WI-1 were nearly completely depleted. For the C_{33} homohopanes, the 22R epimer was nearly undetectable while the 22S epimer still remained in relatively significant abundance. These results are in good agreement with the observation by Munoz [29] in a study of the fate of petroleum biomarkers in a mangrove soil.

Table 3 tabulates diagnostic ratios of major target biomarker compounds (including the ratios of the 22S and 22R epimers of the C_{31} to C_{35} homohopane series relative to C_{30} αβ-hopane) for the most and least degraded samples. For comparison, the values of ratios for the heavily degraded sample EE-T1 from the East Marsh treated plots are also listed in Table 3. Fig. 5 and Table 3 clearly reveal that (1) except to the ratio of C_{27} αββ steranes to C_{29} αββ steranes (0.65 vs. 0.37), the three less degraded samples and the heavy degraded sample EE-T1

Table 3
Comparison of diagnostic ratios of major target biomarker compounds for the less degraded samples EE-C1, EE-C2, and EE-GO and the most degraded samples WI-1 and WI-2[a]

	Less degraded			Heavily degraded, EE−T1	The most degraded		Ref. Oil (AL)
	EE-C1	EE-C2	EE-GO		WI-1	WI-2	
C_{23}/C_{24}	3.14	3.09	2.72	2.88	0.33	1.44	2.42
C_{29}/C_{30}	1.25	1.23	1.22	1.21	1.20	1.16	1.12
C_{29}/C_{29}-nor	4.96	4.69	4.54	4.24	2.30	2.90	4.14
$C_{31}(S)/C_{31}(R)$	1.26	1.23	1.24	1.28	1.52	1.33	1.23
$C_{32}(S)/C_{32}(R)$	1.40	1.50	1.53	1.51	1.99	1.65	1.48
$C_{33}(S)/C_{33}(R)$	1.45	1.45	1.46	1.62	4.46	2.66	1.48
C_{23}/C_{30}	0.13	0.12	0.13	0.12	0.04	0.10	0.18
Ts/Tm	0.93	0.98	0.98	1.01	1.21	1.20	1.01
$\frac{C_{27}\text{-αββ-steranes}}{C_{29}\text{-αββ-steranes}}$	0.67	0.65	0.63	0.37	0.05	0.11	0.77
$\frac{C_{29}\text{-20S-ααα-sterane}}{C_{29}\text{-αββ-steranes}}$	0.40	0.41	0.42	0.41	0.54	0.48	0.41
$C_{31}(S)/C_{30}$	0.62	0.63	0.62	0.63	0.73	0.65	0.63
$C_{31}(R)/C_{30}$	0.49	0.51	0.50	0.49	0.48	0.49	0.50
$C_{32}(S)/C_{30}$	0.37	0.38	0.36	0.38	0.54	0.44	0.39
$C_{32}(R)/C_{30}$	0.26	0.25	0.25	0.25	0.27	0.27	0.27
$C_{33}(S)/C_{30}$	0.24	0.24	0.23	0.25	0.25	0.26	0.24
$C_{33}(R)/C_{30}$	0.16	0.16	0.15	0.15	0.06	0.10	0.16
$C_{34}(S)/C_{30}$	0.14	0.15	0.14	0.14	~0.0	0.07	0.13
$C_{34}(R)/C_{30}$	0.10	0.09	0.09	0.09	~0.0	0.05	0.09
$C_{35}(S)/C_{30}$	0.17	0.17	0.17	0.16	~0.0	0.04	0.16
$C_{35}(R)/C_{30}$	0.10	0.10	0.10	0.09	~0.0	0.01	0.10

[a] C_{23}: C_{23} Tricyclic terpane: C_{24}: C_{24} Tricyclic terpane; Ca_{29}: 17α(H),21β(H)-30-Norhopane; C_{29}-nor: C_{29}18α(H), 21β(H)-30-Norneohopane; C_{30}: 17α(H),21β(H)-Hopane; $C_{31}(S)$: 22S-17α(H),21β(H)-30-Homohopane; $C_{31}(R)$: 22R-17α(H),21β(H)-30-Homohopane; $C_{32}(S)$: 22S-17α(H),21β(H)-30,31-Bishomohopane; $C_{32}(R)$: 22R-17α(H),21β(H)-30,31-Bishomohopane; $C_{33}(S)$: 22S-17α(H),21β(H)-30,31,32-Trishomohopane: $C_{34}(R)$: 22R-17α(H),21β(H)-30,31,32-Trishomohopane; $C_{34}(S)$: 22S-17α(H),21β(H)-30,31,32,33-Tetrakishomohopane; $C_{34}(R)$: 22R-17α(H),21β(H)-30,31,32,33-Tetrakishomohopane; $C_{35}(S)$: 22S-17α(H),21β(H)-30,31,32,33,34-Pentakishomohopane: $C_{35}(R)$: 22R-17α(H),21β(H)-30,31,32,33,34-Pentakishomohopane; Ts: 18α-(H),21β-(H)-22,29,30-Trisnorhopane; Tm: 17α(H), 21β(H)-22,29,30-Trisnorhopane.

demonstrated very close diagnostic ratio values for all target biomarker pair compounds; (2) the smaller tricyclic terpanes such as C_{23} were significantly more degraded than the pentacyclic C_{29} and C_{30} hopanes, resulting in striking decrease in the ratio of C_{23}/C_{30} from 0.18 for the reference oil to 0.04 and 0.10 for the samples WI-1 and WI-2, respectively; (3) C_{30}-αβ-hopane was obviously much more resistant to biodegradation than both the 22S and 22R epimers of C_{34} and C_{35} homohopanes (which had been nearly completely depleted in the sample WI-1); (4) Of particular interest is the observation that the most-abundant C_{30}-αβ-hopane (which is often considered to be a highly biodegradation-resistant biomarker) appeared more sensitive to biodegradation than the 22S epimers of C_{31} and C_{32} homohopanes, indicated by higher ratio values of the C_{31} and C_{32} 22S homohopanes to C_{30}-αβ-hopane for the most degraded sample WI-1 (0.73 and 0.54) compared to the corresponding ratios for the less degraded samples (0.62 and 0.37). But, the relative ratios of C_{31} and C_{32} 22R hopanes to C_{30}-αβ-hopane were almost the same for all samples (~0.50 and 0.26), implying that C_{30}-αβ-hopane had roughly the same biodegradation rate as the 22R epimers of C_{31} and C_{32} homohopanes. This result illustrates that the degradation of biomarkers is not only molecular mass and size dependent, but also stereoisomer dependent.

The C_{29}-18α(H), 21β(H)-30-norneohopane and C_{29}-αββ-stigmastanes (20R and 20S) appeared to be the most biodegradation-resistant terpane and sterane compounds among the target biomarkers examined in this study. As an example, Fig. 6 compares the mass fragmentograms of *m/z* 177 (which is the most characteristic fragment of the 25-demethylated terpanes) for the samples EE-GO, WI-1, and the reference AL oil. Fig. 6 shows that in the reference oil and the sample EE-GO, the C_{29}-18α(H), 21β(H)-30-norneohopane is clearly less abundant than the C_{29}-17α(H), 21β(H)-30-norhopane. The most degraded sample WI-1, however, demonstrated a different distribution pattern of norhopanes with the C_{29}-18α(H), 21β(H)-30-norneohopane being more abundant than the C_{29}-17α(H), 21β(H)-30-norhopane. For purposes of quantitative comparison, the ratios of target biomarkers relative to C_{29}-18α(H), 21β(H)-30-norneohopane were determined and tabulated in Table 4. As Table 4 shows, the ratio values for the samples WI-1 and WI-2 are significantly smaller than the corresponding ratio values for the three less degraded samples without exception.

The steranes in the Metula spill samples were less abundant than the terpane compounds and essentially consist of ααα and βββ C_{27}-cholestanes, C_{28}-ergastanes, and C_{29}-stigmastanes with the lower-molecular-mass C_{21} and C_{22} steranes and C_{27} diasterane being present and quite prominent. Fig. 7 compares the mass fragmentograms of *m/z* 217 for samples EE-C1 and WI-1. Fig. 7 clearly demonstrates that (1) the sterane degradation was in the order of $C_{27}>C_{28}>C_{29}$ steranes. C_{27} steranes were considerably degraded in comparison with C_{28} and C_{29} steranes, resulting in great decrease in ratios of C_{27} αββ-steranes to C_{29} αββ-steranes (decreased to 0.05 and 0.11 for samples WI-1 and WI-2 from 0.63 to 0.77 for the reference oil and the three less degraded samples); (2) four C_{27} diasterane epimers were nearly completely removed; (3) among the four C_{29} sterane epimers, the degradation of C_{29} 20R-αααα-sterane was very significant; (4) the relative ratios of C_{29} 20S-αααα-sterane to C_{29} (20S+20R)-αββ-steranes were determined to be 0.40 and 0.54 (Table 3) for the sample EE-C1 and WI-1, respectively, indicating the degradation of C_{29} steranes in the order of 20R-ααα $\gg$ (20S +20R)-αββ>20S-ααα.

In summary, the degree of biodegradation of biomarker compounds was strongly correlated with their molecular structures. The degradation trends of biomarkers may be proposed as follows: (1) Biomarkers were generally altered in the declining order of importance as: diasteranes>C_{27} steranes>tricyclic terpanes>pentacyclic terpanes>norhapanes~C_{29}αββ steranes; (2) The degradation of steranes was in the order of $C_{27}>C_{28}>C_{29}$ with the stereochemical degradation sequence 20R ααα steranes>20(R+S) αββ steranes>20S ααα steranes; (3) For the pentacyclic terpanes, degradation of $C_{35}>C_{34}>C_{33}>C_{32}>C_{31}$ was apparent with a significantly preferential degradation of the 22R epimers over the 22S epimers; (4) C_{30}-αβ-hopane appeared more degradable than the 22S epimers of C_{31} and C_{32} homohopanes, but had roughly the same biodegradation rate as the 22R epimers of C_{31} and C_{32} homohopanes and was significantly more resistant to degradation than both the 22S and 22R epimers of

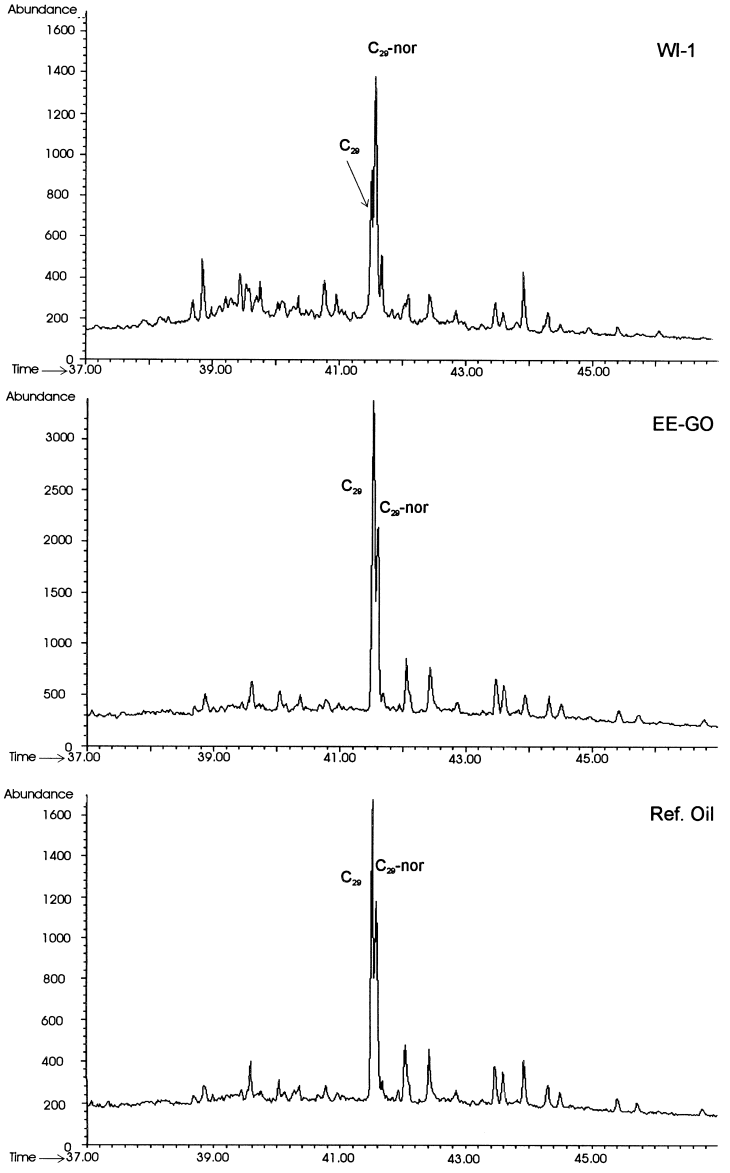

Fig. 6. Comparison of GC–MS fragmentogram at m/z 177 of 25-demethylated pentacyclic terpanes from the most degraded oil sample WI-1 (top), the less degraded oil sample EE-GO (middle), and the reference oil (bottom), illustrating differences in degradation and persistence of biomarkers C_{29}-17α(H),21β(H)-30-norhopane and C_{29}-18α(H),21β(H)-30-norneohopane. Time scales in min.

C_{34} and C_{35} homohopanes; (5) C_{29}-18α(H), 21β(H)-30-norneohopane and C_{29}-αββ 20R and 20S stigmastanes appeared to be the most biodegradation-resistant terpane and sterane compounds, respectively, among the target biomarkers examined in this study.

3.3. Estimation of weathered percentages of the spilled Metula oil

A method using the C_{30}-17α(H), 21β(H)-hopane as an internal conservative reference to estimate the depletion of oil has been developed [33] and used to

Table 4
Comparison of diagnostic ratios of major target biomarkers to $C_{29}18\alpha(H)$, 21β(H)-30-norneohopane for the less degraded samples EE-C1, EE-C2, and EE-GO and the most degraded samples WI-1 and WI-2[a]

	Less degraded			Heavily degraded, EE-T1	The most degraded		Ref. Oil, AL
	EE-C1	EE-C2	EE-GO		WI-1	WI-2	
C_{23}/C_{29}-nor	0.51	0.48	0.48	0.43	0.08	0.24	0.67
C_{24}/C_{29}-nor	0.18	0.15	0.18	0.15	0.25	0.17	0.28
C_{29}/C_{29}-nor	4.96	4.69	4.54	4.24	230	2.90	4.14
C_{30}/C_{29}-nor	396	381	3.72	3.51	1.92	2.51	3.71
$C_{31}(S)/C_{29}$-nor	2.44	241	2.31	2.20	1.41	1.64	2.32
$C_{31}(R)/C_{29}$-nor	1.94	1.95	1.88	1.72	0.92	1.23	1.88
$C_{32}(S)/C_{29}$-nor	1.45	1.43	1.35	1.33	1.03	1.12	1.48
$C_{32}(R)/C_{29}$-nor	I.03	0.96	0.89	0.88	0.52	0.68	0.99
$C_{33}(S)/C_{29}$-nor	0.94	0.91	0.83	0.88	0.49	0.64	0.88
$C_{33}(R)/C_{29}$-nor	0.65	0.83	0.57	0.53	0.11	0.24	0.60
Ts/C_{29}-nor	1.24	1.26	1.20	1.10	0.84	0.99	1.21
Tm/C_{29}-nor	1.33	1.28	1.23	1.09	0.70	0.83	1.20
$C_{27}\alpha\beta\beta/C_{29}$-nor	0.51	0.46	0.43	0.33	0.07	0.11	0.55

[a] C_{29}-nor: C_{29} 18α(H), 21β(H)-30-norneohopane: C_{27} αββ-steranes: C_{27} 20(S+R) αββ-steranes.

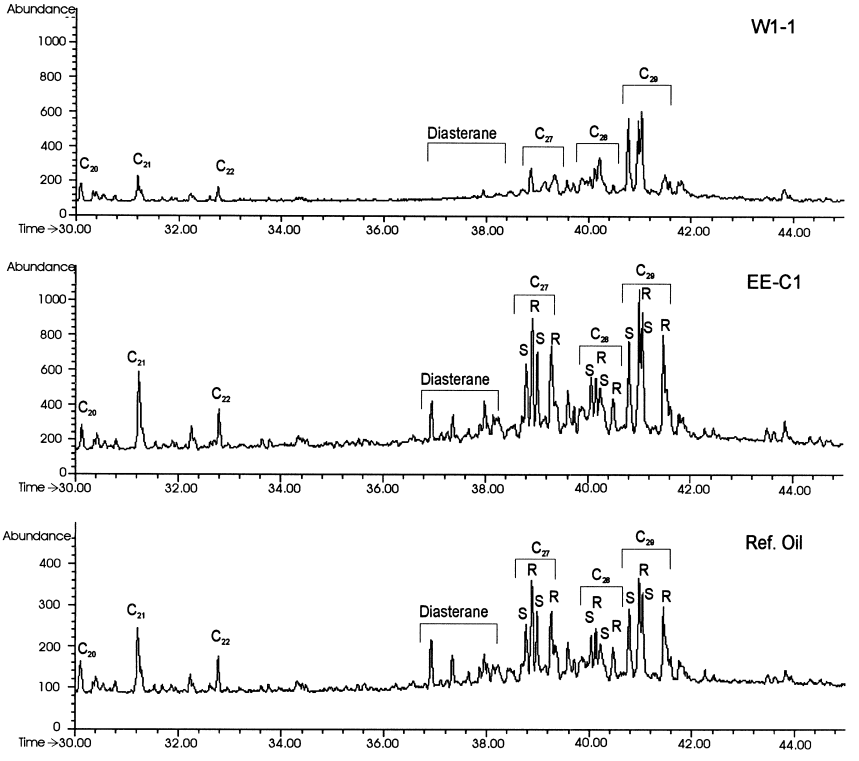

Fig. 7. Comparison of GC–MS fragmentogram at *m/z* 217 of steranes including C_{27} and C_{28} diasteranes from the most degraded oil sample WI-1 (top), the less degraded oil sample EE-C1 (middle), and the reference oil (bottom), illustrating the degradation of steranes in the order of diasteranes>C_{27}steranes>C_{28} steranes>C_{29} steranes. The preferential depletion of C_{27}-C_{29} steranes in the order of 20R ααα>20(S+R) αββ>20S ααα steranes, as a function of their stereochemistry, is also illustrated. Time scales in min.

quantify weathered percentages of residual oil [18]. The equation is expressed as the following:

$$P(\%) = (1 - Cs/Cw) \times 100\%$$

where P is the weathered percentages of the weathered oils; Cs and Cw are the concentrations of C_{30}-αβ-hopane in the source oil and weathered samples respectively.

With this method, the weathered percentages of the residual oils in the Metula samples were estimated to be 25–32% for East Marsh control plot samples, 40–55% for East Marsh treated and West Marsh untreated plot samples (Table 2). Quantitatively, these results show excellent correlation with the TPH, PAH, and biomarker analysis results. The weathered percentages of residual oils in the samples WI-1 and WI-2 can not be directly determined using the method described above, because the C_{30}-αβ-hopane had also been significantly degraded and its concentration was even smaller than that of the reference oil (Table 2). By comparison with other highly weathered oil samples, these two samples are clearly demonstrated to be the most degraded samples, and, therefore, they must have weathered percentages greater than 55%, the highest weathered percentage determined for the East and West Marsh samples.

As discussed above, however, biomarker compounds including C_{30}-αβ-hopane are degradable under severe weathering conditions. Therefore, the calculated weathered percentages may be underestimated because C_{30}-αβ-hopane was used as an internal oil reference which under such circumstances is itself partially biodegraded. For example, the weathered percentages of the three East Marsh untreated plot samples were determined to be 30–38% if C_{29}-18α(H), 21β(H)-30-norneohopane was used as the internal reference. These percentages are clearly higher than the values of 25–32% weathered as determined using C_{30}-αβ-hopane as an internal oil reference. In most cases, however, C_{30}-αβ-hopane is still a preferred choice in estimation of weathered percentages of residual oils, because C_{30}-αβ-hopane is often the most abundant among C_{19} to C_{35} biomarkers and, therefore, can be more readily determined.

References

[1] E.H. Owens, A. Scotland, W. Robson, Report to Environment Canada: Field Observations of Stranded Oil in the Strait of Magellan, Chile — $12\frac{1}{2}$ Years After the 'Metula' Spill, Environment Canada, Ottawa, 1989.

[2] E.H. Owens, O. Sergy, L. Guzman, Z.D. Wang, J. Baker, in: Proceedings of 22nd Arctic and Marine Oilspill Program (AMOP) Technical Seminar, Environment Canada, Ottawa, 1999, pp. 847–864.

[3] J.M. Baker, L. Guzman, P.D. Bartlett, D.I. Little, C.M. Wilson, in: Proceedings of 1993 International Oil Spill Conference, American Petroleum Institute, Washington, DC, 1993, pp. 395–399.

[4] J.M. Baker, L. Guzman, P. Chang, R. Ruiz, in: Unpublished Report (Progress Report 1), Universidad de Magallanes, Chile, 1993.

[5] E.H. Owens, in: Report to Environment Canada: Field Observations at the Punta Espora Sites, Strait of Magellan, Chile — $23\frac{1}{2}$ Years after the 'Metula' Oil Spill, Environment Canada, Edmonton, 1998.

[6] Z.D. Wang, M. Fingas, K. Li, J. Chromatogr. Sci. 32 (1994) 361.

[7] Z.D. Wang, M. Fingas, G. Sergy, Environ. Sci. Technol. 28 (1994) 1733.

[8] D. Straughan, in: Intertidal Ecological Changes after the Metula Oil Spill, University of Southern California, Los Angeles, CA, July, Technical Reports of the Allan Hancock Foundation (no. 4), 1981.

[9] I.R. Kaplan, Y. Galperin, S. Lu, R. Lee, Org. Geochem. 27 (1997) 289.

[10] T.C. Saner, J. Michel, M.O. Hayes, D.V. Aurand, Environ. Int. 24 (1998) 43.

[11] D.S. Page, P.D. Boehm, G.S. Douglas, A.E. Bence, Exxon Valdez oil spill: fate and effects in Alaska waters, in: P.G. Wells, J.N. Butler, J.S. Hughes (Eds.), American Society For Testing and Materials, Philadelphia, PA, 1995, pp. 41–83.

[12] J.W. Short, T.J. Jackson, M.L. Larsen, T.L. Wade, Am. Fisheries Soc. Symp. 18 (1996) 140.

[13] M.C. Kennicutt II, Oil Chem. Pollut. 4 (1988) 89.

[14] A. Farran, J. Grimalt, J. Albaiges, A.V. Botello, S.A. Macko, Mar. Pollut. Bull. 18 (1987) 284.

[15] Z.D. Wang, M. Fingas, S. Blenkinsopp, G. Sergy, M. Landriault, L. Sigouin, P. Lambert, Environ. Sci. Technol. 32 (1998) 2222.

[16] Z.D. Wang, M. Fingas, D. Page, J. Chromatogr. A 843 (1999) 369.

[17] N.M. Fayad, E. Overton, Mar. Pollut. Bull. 30 (1995) 239.

[18] Z.D. Wang, M. Fingas, Environ. Sci. Technol. 29 (1995) 2841.

[19] Z.D. Wang, M. Fingas, M. Landriault, L. Sigouin, Y. Feng, J. Mullin, J. Chromatogr. A 775 (1997) 251.

[20] K.E. Peters, J.W. Moldowan, The Biomarker Guide: Interpreting Molecular Fossils in Petroleum and Ancient Sediments, Prentice Hall, Englewood Cliffs, NJ, 1993.

[21] S.D. Killops, V.J. Howell, Chem. Geol. 91 (1991) 65.
[22] K.E. Poynter, G. Eglinton, Fresenius J. Anal. Chem. 339 (1991) 725.
[23] A.O. Baralcat, A.R. Mustafa, J. Rullkotter, A.R. Hegazi, Mar. Pollut. Bull. 38 (1999) 535.
[24] A.B. Bence, K.A. Kvenvolden, M.C. Kennicutt II, Org. Geochem. 24 (1996) 7.
[25] K.A. Kvenvolden, F.D. Hostettler, P.R. Carlson, J.B. Rapp, C.N. Threlkeld, A. Warden, Environ. Sci. Technol. 29 (1995) 2684.
[26] D.M. McKirdy, R.B. Summons, D. Padley, K.M. Serafmi, C.J. Boreham, H.I. Struckineyer, Org. Geochem. 21 (1994) 265.
[27] D.S. Page, P.D. Boehm, G.S. Douglas, A.B. Bence, W.A. Bums, P.J. Mankiewicz, Environ. Toxicol. Chem. 15 (1996) 1266.
[28] O. Mille, D. Munoz, F. Jacquot, L. Rivet, J.-C. Bertrand, Estuarine, Coastal Shelf Sci. 47 (1998) 547.
[29] D. Munoz, M. Guiliano, P. Doumenq, F. Jacquot, P. Scherrer, O. Mille, Mar. Pollut. Bull. 34 (1997) 868.
[30] P. Chosson, C. Lanau, P. Connan, D. Dessort, Nature 351 (1991) 640.
[31] J.K. Vollcman, R. Alexander, R.I. Kagi, S.J. Rowland, P.N. Sheppard, Org. Geochem. 6 (1984) 619.
[32] N.S. Goodwin, P.J. Park, T. Rawlinson, in: M. Bjoroy et al. (Ed.), Advances in Organic Geochemistry, Wiley, Chichester, 1983, pp. 650–658.
[33] E.L. Bulter, G.S. Douglas, W.G. Steinhauter, R.C. Prince, T. Axcel, C.S. Hsu, M.T. Bronson, J.R. Clark, J.E. Lindstrom, in: R.E. Hinchee, R.F. Olfenbuttel (Eds.), On-site Bioreclamation, Butterworth-Heinemann, Boston, 1991, pp. 515–